
Lagrangian Objective Function Leads to Improved Unforeseen Attack Generalization in Adversarial Training

Mohammad Azizmalayeri¹ Mohammad Hossein Rohban¹

Abstract

Recent improvements in deep learning models and their practical applications have raised concerns about the robustness of these models against adversarial examples. Adversarial training (AT) has been shown effective to reach a robust model against the attack that is used during training. However, it usually fails against other attacks, i.e. the model overfits to the training attack scheme. In this paper, we propose a simple modification to the AT that mitigates the mentioned issue. More specifically, we minimize the perturbation ℓ_p norm while maximizing the classification loss in the Lagrangian form. We argue that crafting adversarial examples based on this scheme results in enhanced attack generalization in the learned model. We compare our final model robust accuracy against attacks that were not used during training to closely related state-of-the-art AT methods. This comparison demonstrates that our average robust accuracy against unseen attacks is 5.9% higher in the CIFAR-10 dataset and is 3.2% higher in the ImageNet-100 dataset than corresponding state-of-the-art methods. We also demonstrate that our attack is faster than other attack schemes that are designed for unseen attack generalization, and conclude that it is feasible for large-scale datasets¹.

1. Introduction

Deep neural networks have been used in many applications and have achieved impressive results in various domains, especially in computer vision tasks such as image classification, autonomous vehicles, and face recognition (Lin

¹Department of Computer Engineering, Sharif University of Technology, Tehran, Iran. Correspondence to: Mohammad Azizmalayeri <azizmalayeri@ce.sharif.edu>, Mohammad Hossein Rohban <rohban@sharif.edu>.

Preprint

¹Code is available at https://github.com/rohban-lab/Lagrangian_Unseen.

et al., 2018; Wang & Deng, 2020). But there are still a lot of security-based concerns about them as it has been demonstrated that these networks are not sufficiently robust against different types of adversarial examples (Akhtar & Mian, 2018; Szegedy et al., 2014). Adversarial examples are data points that are slightly perturbed and optimized to deceive a network. Numerous defenses have been developed against adversarial examples, but the issue has not yet been completely solved as the proposed methods lead to robustness against a limited number of threat models with specific conditions.

Variants of adversarial training (AT) (Madry et al., 2018) are currently state-of-the-art algorithms among empirical defenses. AT tries to solve an optimization problem of minimizing loss of the network f parameterized by θ based on adversarial examples $x_i + \delta_i$. The perturbation δ_i is obtained by maximizing the network loss for $x_i + \delta_i$. In order to make the perturbation imperceptible, δ_i could be norm bounded. Therefore, AT briefly involves:

$$\min_{\theta} \sum_i \max_{\delta \in \Delta} \ell(f_{\theta}(x_i + \delta), y_i),$$

where $\ell(\cdot)$ is the loss function, and Δ is the set of feasible perturbations. The outer minimization can be done using the stochastic gradient descent algorithm, but the challenging part often involves solving the inner maximization. It has been empirically observed that the final model will be robust mainly against perturbations within Δ , but almost fails under other threat models (Ilyas et al., 2019).

To tackle this challenge, two strategies were considered in the literature: training against union of perturbation sets (Maini et al., 2020), or using a more perceptually aligned metric to define the perturbation set, Δ (Laidlaw et al., 2020). Along the first strategy, (Maini et al., 2020) proposed an attack that is updated based on the gradient from the worst case error of $\{\ell_1, \ell_2, \ell_{\infty}\}$ attacks in each iteration. Such methods do not still generalize to imperceptible attacks that are not norm bounded (Laidlaw et al., 2020). As an alternative, it was proposed to broaden Δ to contain more general attacks. For instance, (Laidlaw et al., 2020) recently used a deep neural network to bound the attack based on the network embedding, which is called the LPIPS distance and is believed to be a more perceptual metric. The constrained

version of their algorithm is computationally demanding, so they proposed a Lagrangian penalty in designing the attack. This idea led to promising results on unseen attacks.

We will build upon this work and show that the Lagrangian nature of the loss plays a more important role in unseen attack generalization than the LPIPS distance. We observed that the results improve further if we replace the LPIPS in the Lagrangian setting with the ℓ_2 distance! We give some theoretical insights on a possible explanation for this observation. It has also been pointed out that due to the deep neural network adversarial fragility, the LPIPS metric has certain shortcomings in modeling the perceptual distances (Kettunen et al., 2019).

We also note that in the ideal case, the distance metric should not have any a priori bias towards specific δ . This fact brings out an issue with the LPIPS distance. As demonstrated in Fig. 1, LPIPS uses the ℓ_2 norm difference of outputs of internal convolutional layers of a pre-trained network for calculating the distance between x_i and $x_i + \delta$. Internal layers of the networks are mainly sensitive to foreground, i.e. parts of the image that contain the target object. As a result, changes in the background of the object do not often change the internal layers a lot. This would encourage the perturbation to make changes in the background and cause some natural bias in the attack. We will discuss this bias in more details in section 4.

According to these reasons, we suggest $\|\delta\|_2$ as the distance metric since it does not impose such biases in the attack. Closely related to this attack, C&W attack (Carlini & Wagner, 2017) also tries to find the minimal perturbation that can fool the classifier by adding a second term to the loss function to avoid large perturbations. However, the main difference of (Carlini & Wagner, 2017) with our work is in adjusting the weight, λ , that is multiplied by the norm in the loss. For each instance, C&W attack initializes λ with a large value and gradually decreases it until it reaches a successful adversarial example. This gives us the minimal successful perturbation, which sounds reasonable for the test time. But it has two disadvantage in the training time. First, searching over λ makes this attack infeasible for large-scale datasets. The second disadvantage is the fact that other attacks do not necessarily generate minimal perturbations, and hence C&W does not make the model robust against such attacks. Therefore, we propose to use a fixed schedule of λ for all samples to avoid these problems. More importantly, we argue that based on the envelope theorem, a *fixed* λ places an upper bound on the gradient of the loss with respect to the perturbation budget, ϵ , while also prevents δ from be overly small on average. Therefore, we hypothesize that fixing λ prevents the loss function to change drastically across slightly different perturbation sets, and results in improved unforeseen attack generalization.

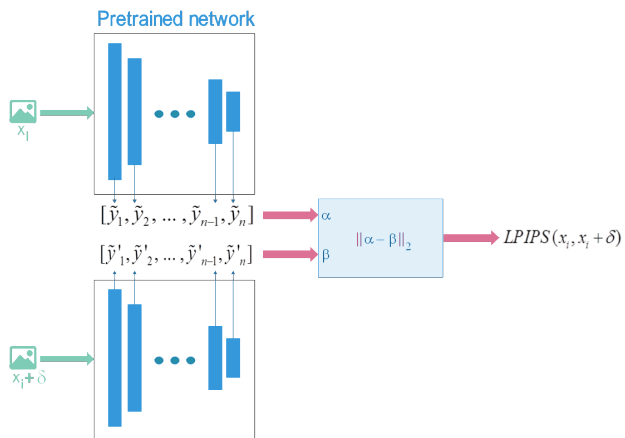


Figure 1. LPIPS distance. First, outputs of convolutional layers of a pretrained network for each image is calculated (y_i, y'_i) and normalized using height and width ($\tilde{y}_i, \tilde{y}'_i$). Next, ℓ_2 norm difference between \tilde{y} and \tilde{y}' is calculated that gives LPIPS distance between images.

In summary, we propose to use Lagrangian objective function with a fixed multiplier to achieve better average accuracy against unforeseen attacks. We give some theoretical insights to support the use of such attacks in AT. We also note that the mentioned attack is feasible for large datasets. We finally compare our method with state-of-the-art methods against attacks that were not used during training, and will demonstrate that our method is outperforming state-of-the-art.

2. Related Work

Adversarial attacks and defenses have attracted a lot of attention in recent years. Attacks are being proposed sequentially while defenses try to confront them and this loop always exists (Uesato et al., 2018; Athalye et al., 2018a). Here, we explore some popular adversarial attacks and empirical defenses.

2.1. Adversarial attacks

One of the first successful attacks against deep neural networks was the Fast Gradient Sign Method (Goodfellow et al., 2015) that used input gradient signs to craft the adversarial perturbation. (Madry et al., 2018) tried to perform FGSM iteratively inspired by (Kurakin et al., 2017) and proposed Projected Gradient Descent (PGD) that moves iteratively along the gradient direction, and scale the perturbation using the ℓ_p norms. MI-FGSM (Dong et al., 2018) used momentum to modify the gradient direction in each step of designing the perturbation. (Rony et al., 2020) used the Lagrange method, similar to the C&W attack, (Carlini

& Wagner, 2017) to generate minimal perturbations, except that they modify the Lagrange weight in each iteration in a way that their distance metric is better satisfied. DeepFool attack assumed that the classifier is linear in a neighborhood of each example and tried to reduce the model’s accuracy by moving the example toward the nearest linear border (Moosavi-Dezfooli et al., 2016). ℓ_0 attacks such as PGD₀ and CornerSearch, deceive network with changing minimal pixels (Croce & Hein, 2019; Modas et al., 2019).

As an alternative to the ℓ_p norm bounded attacks, Wasserstein distance for adversarial robustness was introduced by (Wong et al., 2020) as a better distance for imperceptible perturbations. However, their proposed Sinkhorn iterations for projecting onto the Wasserstein ball is computationally expensive and prohibitive in large datasets. Perceptual metrics such as SSIM (Zhou Wang et al., 2004) and LPIPS (Zhang et al., 2018) are another alternatives for the standard ℓ_p norms. For instance, (Laidlaw et al., 2020) proposed the LPA and PPGD attacks using the LPIPS distance, Fig. 1, for crafting perturbations that are not visible and recognizable for human.

As the perturbation set is broader in such attacks, compared to the traditional ℓ_p attacks, one would expect robustness against unseen attacks once the model is trained using those attacks. In order to check the model’s accuracy against unseen attacks, (Kang et al., 2020) proposed JPEG, Fog, Snow, and Gabor attacks that we will also use to compare our final model’s accuracy with the rest. StAdv (Xiao et al., 2018) and RecolorAdv (Laidlaw & Feizi, 2019) are also recently proposed as other alternative adversarial attacks. StAdv makes local spatial transformation of each input pixel adversarially, and RecolorAdv maps the pixel original color to a perceptually indistinguishable color to fool the classifier. We will also evaluate our model based on these attacks.

2.2. Empirical Defenses

Several defense methods have been proposed in the literature, but as pointed out in (Athalye et al., 2018b), many of these defenses suffer from a phenomenon called “gradient masking” and “gradient obfuscation.” Perhaps the most effective defenses are variants of adversarial training (Madry et al., 2018). This includes training with PGD adversarial examples. Our work is also concentrated on the same concept.

Adversarial training on multiple perturbations is also investigated to reach robustness against multiple threat models (Tramèr & Boneh, 2019; Maini et al., 2020), but our work is more general and aims to reach robustness against all unseen attacks. Adversarial training can also be combined with self supervised learning methods to improve robustness (Kim et al., 2020; Chen et al., 2020). But in this work, we try to improve the base adversarial training, which could

lead to improvement of its variants. Finally, note that there could be a trade-off between standard accuracy and robust accuracy (Tsipras et al., 2019). Therefore, to have a fair evaluation, one has to compare the adversarial accuracy of different methods, under the same or similar clean accuracy.

3. Proposed approach

The main contribution of our work is proposing an attack that is specifically designed to be used in adversarial training (Madry et al., 2018). In our proposed attack, we attempt to maximize $\ell(f_\theta(x_i + \delta), y_i)$, where f is the network parametrized by θ that classifies samples x_i with labels y_i , and we use (Carlini & Wagner, 2017) margin loss as $\ell(\cdot)$. In order to force the perturbation δ to be small, we use the Lagrangian formulation and add a penalty term $\|\delta\|_2$ to the loss function. We will empirically show that this simple modification boosts the generalization of the trained model to new unforeseen threat models.

As mentioned in section 1, the penalty term should preferably be unbiased against penalizing specific perturbations at the training time. Otherwise, it will cause overfitting to the training attack and prohibits the generalization of the classifier to unforeseen threat models. To consider this issue, we suggest $\|\delta\|_2$ as the penalty term, since it treats all pixels of the image in the same way. Other differentiable ℓ_p norms can also be used for this purpose, but the optimization may become harder. So our final objective function for generating perturbations would be:

$$\max_{\delta} \ell(f_\theta(x_i + \delta), y_i) - \lambda \|\delta\|_2,$$

and λ is the constant Lagrange multiplier that determines the compromise between the first and second terms. The penalty term acts as a “perturbation decay” in gradient descent (GD) iterations, and prevents the input gradients from over-enlarging in each iteration.

At least five steps are required to perform this optimization since we maximize the loss and minimize the distance simultaneously. Using five steps, we can start with a smaller λ to move a sample in a space with maximum loss without worrying about the distance. In the following steps, λ is increased to make the ℓ_2 distance smaller, and simultaneously reduce α to make sure that more minor changes are made in that step, and the sample is still adversarial. To ensure that decreasing α reduces the amount of changes, the gradient scale in different steps should be the same. So, we normalize the gradients in each step. Our attack is summarized in Alg. 1.

Next, using our proposed attack $\delta_{\text{Lag},i}$, we perform adversarial training in the form of:

$$\min_{\theta} \sum_i \ell(f_\theta(x_i + \delta_{\text{Lag},i}), y_i)$$

Algorithm 1 Our adversarial attack designed specifically for adversarial training

Input: network classifier f_θ , data x , label y

Parameters: number of iterations N , initial step size α , initial Lagrange multiplier λ , perturbation initialization variance σ^2 (default 0.01), decay parameter c (default 0.1)

Output: perturbation δ

$\delta \sim \mathcal{N}(0, \sigma^2)$

for $i = 0$ **to** $N - 1$ **do**

$\lambda' \leftarrow \lambda \times e^{1-i/N}$

$\alpha' \leftarrow \alpha \times c^{i/N}$

$g \leftarrow \nabla(\ell(f_\theta(x + \delta), y) - \lambda' \|\delta\|_2)$

$g \leftarrow g / \max(|g|)$

$\delta \leftarrow \delta + \alpha' g$

end for

Return: δ

and we use SGD to minimize the total loss. Note that there could be a trade-off between standard accuracy and robust accuracy (Tsipras et al., 2019). Therefore, by decreasing λ and allowing larger perturbation sizes, one would expect a lower clean accuracy. For this reason, the training attack parameters should be adjusted in a way that model reaches a satisfactory standard accuracy.

3.1. Relation to Earlier Work

Here, we discuss the connection between our method and some relevant earlier work such as MART (Wang et al., 2020) and instance adaptive method (Balaji et al., 2019). MART investigated the effect of misclassified and correctly classified examples on the robustness of adversarially trained models. They suggested that misclassified examples and correctly classified examples should be treated differently during training. Instance adaptive method increased the perturbation margin for each sample specifically until the sample is correctly classified. They trained the network using the clean loss for misclassified examples, and adversarial loss for correctly classified examples.

Our work is a generalization of these methods. Our proposed attack uses a constant Lagrange multiplier that causes larger perturbations for confidently classified examples and approximately no perturbation for examples that are confidently misclassified. To empirically demonstrate this point, we plotted $\|\delta\|_2$ against the probability of belonging to the correct class using the classifier output, for each sample in the CIFAR-10 test dataset. Here, we considered δ be obtained using PGD (ℓ_2, ℓ_∞) (Madry et al., 2018), δ_{Lag} . (ours), and Fast-LPA used in PAT (Laidlaw et al., 2020). Fig. 2

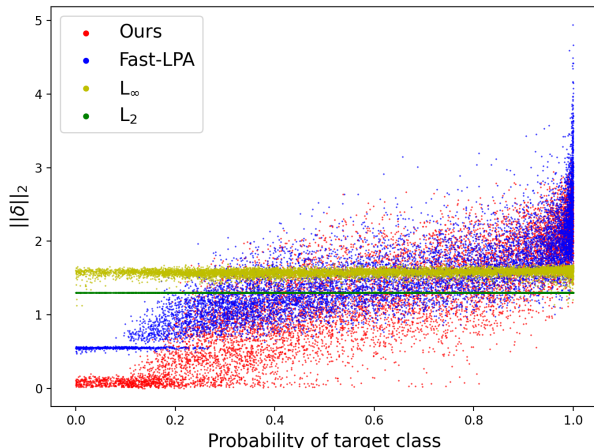


Figure 2. ℓ_2 norm of perturbations generated using our attack, PGD (ℓ_2, ℓ_∞) and Fast-LPA vs. probability of the correct class that is estimated by the network for clean examples in the CIFAR-10 test dataset.

shows the plot. Based on this figure, ℓ_2 norm of perturbations for PGD attacks are approximately constant, but in our attack and Fast-LPA that are using the Lagrangian formulation, it has direct relationship with classifier confidence of correctly classifying the example. The advantage of this adaptive perturbation magnitude is discussed in (Balaji et al., 2019).

3.2. Theoretical Insights

Here, we provide some theoretical insights that support the Lagrangian formulation. Let

$$U_\Delta := \max_{\delta \in \Delta} \ell(f_\theta(x + \delta), y),$$

which is the maximum loss at the input x for a custom threat model Δ . We let δ_Δ denote the perturbation that results in U_Δ . Also, let

$$L_2^\epsilon := \max_{\delta} \ell(f_\theta(x + \delta), y) \quad \text{s.t.} \quad \|\delta\|_2 \leq \epsilon.$$

As mentioned above, we use the Lagrangian to solve this problem that gives us

$$\delta_{\text{Lag}}^* := \arg \max_{\delta} \ell(f_\theta(x + \delta), y) - \lambda \|\delta\|_2.$$

We next define $\Delta\epsilon$ as:

$$\Delta\epsilon := \|\|\delta_\Delta\|_2 - \|\delta_{\text{Lag}}^*\|_2\|$$

On the other hand, using the envelope theorem (Milgrom & Segal, 2002), we have:

$$\frac{\partial L_2^\epsilon}{\partial \epsilon} = \lambda,$$

for the ϵ that corresponds to λ that is the constant Lagrange multiplier in our method. Now, using the Taylor series, we have:

$$U_{\Delta} \leq L_2^{\|\delta_{\Delta}\|_2} \leq L_2^{\|\delta_{\text{Lag}}^*\|_2} + \lambda \cdot (\Delta\epsilon) + o(\Delta\epsilon)$$

So if $\Delta\epsilon$ is small, knowing that λ is fixed, bounding $L_2^{\|\delta_{\text{Lag}}^*\|_2}$ using adversarial training with our proposed attack would be equivalent to bounding U_{Δ} that is related to the attack model Δ that has slightly different ℓ_2 norm than what is considered in the training. In section 4.6, this proof is discussed more practically.

4. Experiment

4.1. Setup

To this end, we proposed a new adversarial attack for training time which aims to be robust against unseen threat models. To evaluate our method, we adversarially trained the ResNet-18 model using our attack on CIFAR-10 (Krizhevsky & Hinton, 2009), and the ResNet-34 on the ImageNet-100 dataset (100-class subset of ImageNet (Russakovsky et al., 2015) containing every 10th class by the WordNet ID). We compare the robust accuracy of our method with other state-of-the-art methods against attacks that are used during training and a number of unseen attacks for each of these datasets. For training, we used standard techniques such as learning rate decay and warm-up to make the convergence faster. More specifically, following (Laidlaw et al., 2020), the learning rate for weight updates in SGD is set to 0.1 initially, and reduced by a factor of 0.1 at epochs 70 and 90 in CIFAR-10. For the ImageNet-100, it is initially set to 0.1 and reduced by a factor of 0.1 at epochs 30, 60, and 80. The models are trained for 100 and 90 epochs in CIFAR-10 and ImageNet-100, respectively. The warm-up step is pre-training the networks with clean data samples for three epochs. We applied the same techniques in training rest of the models to have a fair comparison. In order to make the robust accuracy of different models comparable, we tuned the attack hyperparameters in each method to get similar/same clean accuracy. This has been achieved by changing the bounds on the perturbation size of each method such that we reach a similar standard accuracy for all the models.

4.2. Baseline Methods

We compare our method with the best methods that have reached acceptable and competitive robust accuracies. For CIFAR-10 dataset, we use TRADES (ℓ_{∞}) (Zhang et al., 2019) as a method that considered the trade-off between standard and robust accuracy, and MART (Wang et al., 2020) since it treats misclassified examples differently and adversarial training (AT) with PGD (ℓ_{∞}, ℓ_2) (Madry et al., 2018)

with or without early stopping (ES). We also compare with adaptive methods such as IAAT (Balaji et al., 2019), MMA (Ding et al., 2020), and DDN (Rony et al., 2019). In addition, MSD (Maini et al., 2020), and PAT (Laidlaw et al., 2020) tried to reach robustness against multiple perturbations and perceptual attacks that we also compare against. All methods have been used with similar settings introduced for that method. Only in some cases for a fairer comparison, the perturbation budget size of training has been increased to achieve a better robust accuracy at the cost of reducing clean accuracy. For example, we trained the AT- ℓ_2 model with $\epsilon = 1.3$ and AT- ℓ_{∞} with $\epsilon = 10/255$.

Among the mentioned cases, only adversarial training with PGD and Fast-LPA (PAT method) have been examined with ImageNet dataset, due to shortage of computational resources. For a better comparison, we also consider adversarial training with JPEG attack (Kang et al., 2020). Prior work (Kang et al., 2020; Laidlaw et al., 2020) have demonstrated that the models that are trained using the JPEG attack, as opposed to other attacks such as Elastic, Fog, Gabor, Snow, RecolorAdv, and StAdv, have better generalization against unseen attacks. We also do not use training with the union of attacks for two reasons. First, (Laidlaw et al., 2020) demonstrated that the PAT method is more robust than optimizing the model with a random attack from the union of attacks or the average or worst case loss. Second, it is inconsistent with our goal of examining the final model with unseen attacks since this method assumes that all types of possible attacks are known.

However, to examine whether the instance adaptive perturbation bound has played a role in improving the results, as demonstrated in Fig. 2 and discussed in section 3, we train a model using PGD- ℓ_{∞} and another using PGD- ℓ_2 with different perturbation bounds based on the probability of correct class given the clean examples. For this goal, we set the thresholds $\{0.1, 0.25, 0.5\}$ to divide $[0, 1]$ interval for probability of the correct class into 4 sub-intervals, and set the maximum allowable perturbation in these sub-intervals to 0.03ϵ , 0.3ϵ , 0.55ϵ , and ϵ , respectively. We name these methods Threshold- ℓ_{∞}/ℓ_2 and we test them only on CIFAR-10 dataset, for the sake of performing an ablation study.

4.3. Unforeseen Attacks

To evaluate models that are trained on CIFAR-10, we use the attacks that are employed in the training time (PGD(ℓ_{∞}, ℓ_2), LPA), and unseen attacks that are widely used in earlier work. (Kang et al., 2020) suggested 5 different types of attacks, including Elastic, JPEG, FOG, Gabor, and Snow, as unseen attacks and calibrated maximum distortion size for some of them in CIFAR-10, and all of them in the ImageNet-100 dataset. At the test time, we use the calibrated ones with maximum distortion size of ϵ_3 for CIFAR-10, and ϵ_2 for

Table 1. Test robust accuracy of our model along with other models against training attacks and unseen attacks in the CIFAR-10 dataset. Clean accuracy and robust accuracy of our model and other state-of-the-art models against LPA (bound=0.5, steps=200), ℓ_∞ (bound=8/255, steps=40), ℓ_2 (bound=1.0, steps=40), RecolorAdv (bound=0.06, steps=100), StAdv (bound=0.05, steps=100), Elastic (bound=0.5, steps=50), JPEG (bound=0.125, steps=50), Gaussian noise (mean=0.0, variance=0.05), Gaussian Blur (kernel size=5, sigma=1.5), and PGD₀ (bound=10, steps=20) are reported in this table. Unseen mean shows average accuracy against unseen attacks and union mean shows average accuracy against all the attacks.

Training method	Clean	Training attacks			Unseen attacks							Unseen mean	Union mean
		LPA	ℓ_∞	ℓ_2	Recolor	StAdv	Elastic	Jpeg	Noise	Blur	PGD ₀		
Trades ℓ_∞	79.54	0.18	51.91	38.66	60.57	24.22	37.56	36.12	47.70	56.45	50.91	44.79	40.43
MART ℓ_∞	80.01	0.29	54.03	38.32	59.61	18.45	38.63	36.87	42.23	54.85	50.33	43.00	39.36
MSD	80.62	1.69	48.69	49.11	55.34	14.86	33.88	53.86	42.56	57.71	70.19	46.91	42.79
DDN ℓ_2	72.18	17.92	42.44	46.34	29.06	3.65	35.36	34.44	51.32	46.23	52.67	36.10	35.94
MMA ℓ_2	82.07	2.67	47.74	50.79	49.97	27.74	34.57	55.20	39.67	63.66	45.32	45.16	41.73
IAAT ℓ_∞	82.53	14.97	47.89	38.34	39.79	2.74	42.98	35.84	69.29	60.55	45.83	42.43	39.82
AT ℓ_2	78.59	1.20	45.60	51.48	53.57	19.73	26.67	60.14	52.30	58.35	63.30	47.72	43.23
AT ℓ_2 ES	74.90	1.97	47.88	53.38	57.98	24.87	33.66	58.48	49.74	56.62	60.06	48.77	44.46
Threshold ℓ_2	78.08	1.17	43.64	50.38	56.09	25.93	26.18	57.33	52.21	59.11	63.10	48.56	43.51
AT ℓ_∞	79.98	0.30	53.41	38.45	58.94	16.17	34.28	38.57	36.61	54.08	47.25	40.84	37.81
AT ℓ_∞ ES	79.36	0.42	53.31	38.77	58.98	17.62	33.76	39.21	40.72	54.13	49.25	41.95	38.62
Threshold ℓ_∞	80.90	0.29	51.45	37.69	62.59	22.31	38.26	33.8	50.08	56.62	47.98	44.52	40.11
PAT	80.31	5.14	43.19	46.19	66.45	45.31	34.02	48.16	39.06	55.89	57.22	49.44	44.06
<i>Ours</i>	80.43	1.50	48.12	54.17	69.14	41.57	36.83	61.37	52.93	62.36	63.37	55.37	49.14

ImageNet-100 based on (Kang et al., 2020) calibration. We also use StAdv (Xiao et al., 2018), RecolorAdv (Laidlaw & Feizi, 2019), PGD₀ (Croce & Hein, 2019), Gaussian noise, and Gaussian blurring to make unseen attacks more comprehensive. These attacks are selected to cover a diversity of corruptions. For the ImageNet-100 dataset, we use the same attacks that are mentioned above except PGD₀ since it has not been examined on the ImageNet. Note that attack parameters are selected following parameters that are widely used in earlier work or instructions of the paper that proposed the attack. Detailed information about attacks are mentioned in the caption of Tables 1 and 2.

4.4. Adversarial Accuracy

Results of evaluating our method and other mentioned methods against training and unseen attacks are listed in Table 1 for CIFAR-10, and Table 2 for the ImageNet-100 dataset. These results demonstrate that our method is more robust than others against unseen attacks and union of unseen and training attacks on average. In CIFAR-10, our model has 5.93% and 4.68% higher average robust accuracy than others against unseen attacks and union of attacks, respectively. In ImageNet-100, our model also reaches 3.16% and 3.11% higher robustness accuracy against unseen attacks, and union of attacks, respectively.

We note that (Threshold- ℓ_∞) and (Threshold- ℓ_2) have higher

robustness than PGD- ℓ_∞ and PGD- ℓ_2 , respectively, that demonstrates the influence of lower perturbation margin for misclassified examples on unseen attack generalization. As explained in section 3, our Lagrangian method with a fixed multiplier generally does the same thing.

4.5. Computational Efficiency

Our proposed attack is also computationally efficient. Since the comparison of execution time depends on the exact GPU/CPU that is used for training, mentioning numbers for the training time does not help much in practice. Therefore, we only compare the execution time order. Each iteration of our attack is approximately equal to one iteration in a PGD attack in terms of the running time. Considering that we use only 5 iterations, the execution time of our attack is almost equivalent to the PGD-5 attack.

We note that PGD is usually used with 10 or more iterations at the training time to achieve robustness against perturbations with larger ℓ_p -radii (Andriushchenko & Flammarion, 2020). So our attack takes about half the time required for the conventional PGDs. Fast-LPA attack that is used in PAT, generates perturbation in 10 iterations, while we use only 5. However, it also computes the LPIPS distance in each iteration that makes each iteration more time-consuming, about 1.2 times for Fast-LPA with AlexNet. So our attack is also much faster than the Fast-LPA. Other attacks such

Table 2. Test robust accuracy of our model along with other models against training attacks and unseen attacks in the ImageNet-100 dataset. Clean accuracy and robust accuracy of our model and other state-of-the-art models against LPA (bound=0.25, steps=200), ℓ_∞ (bound=4/255, steps=40), ℓ_2 (bound=4.0, steps=40), RecolorAdv(bound=0.06, steps=100), StAdv(bound=0.05, steps=100), Elastic(bound=0.5, steps=50), JPEG(bound=0.125, steps=50), Fog(bound=256, steps=50), Gabor(bound=0.125, steps=50), Snow(bound=0.125, steps=50), Gaussian noise (mean=0.0, variance=0.05), and Gaussian Blur (kernel size=5, sigma=1.5) are reported in this table. Unseen mean shows average accuracy against unseen attacks and union mean shows average accuracy against all the attacks.

Training method	Clean	Training attacks				Unseen attacks								Unseen mean	Union mean
		LPA	ℓ_∞	ℓ_2	JPEG	Recolor	StAdv	Elastic	Fog	Gabor	Snow	Noise	Blur		
AT ℓ_2	70.14	2.30	40.54	40.07	46.72	21.67	16.58	40.70	17.54	50.62	34.7	25.06	60.67	33.44	33.10
AT ℓ_∞	70.28	0.02	50.35	13.24	7.74	32.51	14.41	46.38	12.96	55.20	45.36	8.35	58.60	34.22	28.76
JPEG	72.43	0.53	46.21	35.88	65.12	37.67	8.61	44.44	14.46	54.60	36.44	31.93	64.72	36.61	36.72
PAT	70.11	6.42	43.14	43.29	49.28	32.10	34.54	46.92	16.17	52.92	39.36	18.66	58.09	37.35	36.74
Ours	69.95	8.93	46.47	46.59	52.16	34.32	35.26	47.86	17.16	54.24	42.84	29.43	62.95	40.51	39.85

Table 3. Average and standard deviation of effective λ in models trained with CIFAR-10 for samples in this dataset.

model	Avg. λ	Std. λ
DDN ℓ_2	1.14	0.84
MMA ℓ_2	1.65	1.72
IAAT ℓ_∞	0.96	1.99
AT ℓ_2	0.86	0.87
AT ℓ_∞	0.63	0.54
PAT	0.76	0.9
Ours	0.38	0.43

as JPEG, are also computationally worse than ours, since they use more iterations or each iteration of their method consumes more time than ours. This makes our method scalable for training large models on large datasets.

4.6. Remarks

Effective λ :

To validate our theoretical insights furthermore, we estimated the effective average λ , which is defined as the derivative of adversarial loss with respect to ϵ , for some of the CIFAR-10 models that are investigated in Table 1. Based on the results in Table 3, our method has the lowest such λ and based on our insights in section 3.2, lower λ causes a tighter upper bound on the loss from unforeseen attacks and improves the accuracy against them, which is consistent with our experiments in section 4.4.

Signed vs. pure input gradients:

We note that using the pure input gradients, as opposed to the signed gradient, in the iterative updates, would help to craft stronger perturbations even in the ℓ_∞ threat model. To demonstrate this, we test ℓ_2 and ℓ_∞ adversarially trained models against PGD-40 (ℓ_∞) and a modified version of PGD-40 (MPGD-40) that does not take the sign from gradi-

Table 4. Testing ℓ_2 and ℓ_∞ adversarially trained models against ℓ_∞ attacks with small and large bounds, using 40 iteration for optimizing the perturbations. In CIFAR-10, we set small=8/255 and large=16/255 and in ImageNet-100, we set small=4/255 and large=8/255. MPGD is our modified version of PGD without using the gradient sign. Step size for each method is selected with a grid search.

Dataset	Model	PGD (small)	MPGD (small)	PGD (large)	MPGD (large)
CIFAR-10	AT ℓ_2	45.6	43.05	17.95	10.62
	AT ℓ_∞	53.41	52.06	27.19	24.01
ImageNet-100	AT ℓ_2	40.54	38.91	17.56	15.13
	AT ℓ_∞	50.5	49.84	31.15	27.76

ents but normalizes them between -1 and 1 to bring gradients from different samples in the same scale. Results listed in Table 4 demonstrate that this small change has made the attack stronger and confirms our claim.

LPA bias towards the background:

Next, we notice that the LPA attack is more biased to perturb pixels in the background of the input image. Here, we practically demonstrate that using LPIPS instead of $\|\delta\|_2$ makes perturbations to be focused more on the background of the image. To validate this claim, we use segmentation as a tool to separate the background and foreground of the input image. We then calculate the ratio of total perturbations in the foreground to total perturbations in the background. For this goal, we used the deep networks with the same architecture to (Lehman, 2019) for CIFAR-10, and (Zagoruyko & Komodakis, 2017) for ImageNet-100 to separate background and foreground in clean images. This gives us an estimation of the probability of a pixel being part of the main object. Segmentation results for CIFAR-10 are shown in Fig. 3, which shows a decent performance in spite of low

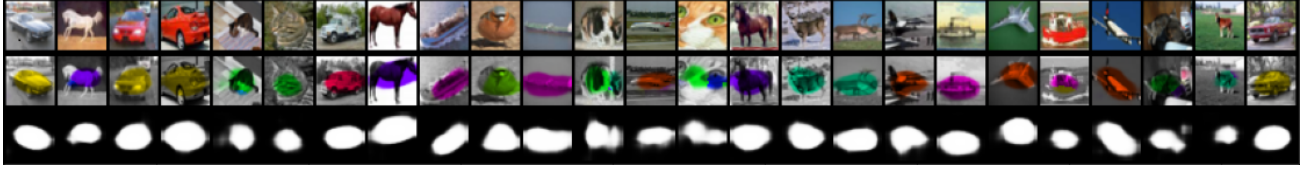


Figure 3. Segmentation results for CIFAR-10. First row shows some images from the CIFAR-10 dataset and the next rows is those images after separating background from the foreground. Last row also shows the segmentation mask for the images.

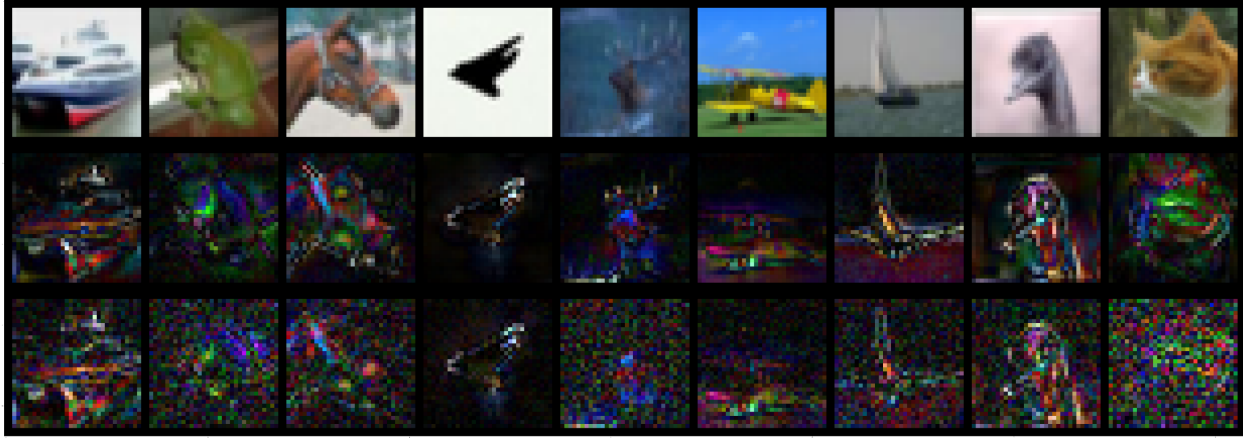


Figure 4. Comparison of the generated perturbations using LPIPS distance, and $\|\delta\|_2$ as the penalty term. First row shows some images from CIFAR-10 dataset, second row shows generated perturbation for images in first row using $\|\delta\|_2$ as the distance metric, and the third row is the generated perturbation using the LPIPS distance.

resolution images.

Using the segmentation results, we define F2B as a measure to determine the ratio of total perturbations in the foreground to total perturbations in the background as:

$$F2B(\delta) := \frac{\sum_i (|\delta_i| \times p_i) / \sum_i p_i}{\sum_i (|\delta_i| \times (1 - p_i)) / \sum_i (1 - p_i)},$$

where p_i is the calculated probability of pixel i belonging to the foreground, and δ_i is the perturbation value at the same pixel. For CIFAR-10, average F2B is 1.42 for LPIPS, while it is 1.69 for $\|\delta\|_2$. For ImageNet-100, it is 1.06 and 1.16, respectively. This confirms higher focus of the LPA perturbation in the background than the ℓ_2 norm. To make this more clear, output perturbation of these attacks are shown in Fig. 4 for some sample images from the CIFAR-10 dataset. It is obvious that generated perturbations with LPIPS as the distance metric has made more changes in the background than generated perturbations with the ℓ_2 norm.

C&W attack for adversarial training:

As our proposed attack is similar to the C&W attack, we also investigate adversarially trained model with the C&W attack. Since C&W is extremely time-consuming, we use only the first three classes of the CIFAR-10 dataset. We evaluate the resulting models against PGD- ℓ_2 with various bounds.

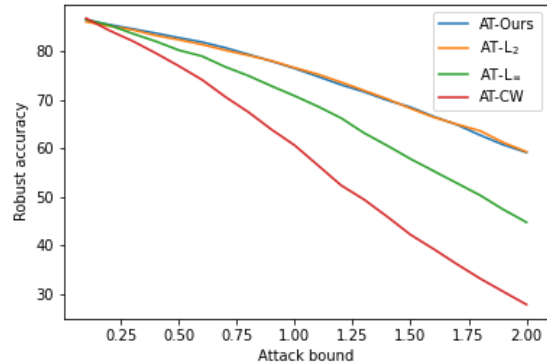


Figure 5. Comparison of robust accuracy for C&W-trained model with three other methods against PGD- ℓ_2 on three first classes of CIFAR-10 dataset. PGD- ℓ_2 bound is gradually increased from 0.1 to 2.

Based on the Fig. 5, robust accuracy of the C&W-trained model decreases more than other models as the allowable range of perturbation increases, due to training of the model with minimally perturbed examples.

Comparison against other perturbation budgets:

Table 5. Evaluating five different methods trained on CIFAR-10 against PGD attacks with three different bounds.

Training method	ℓ_2			ℓ_∞		
	0.75	1.00	1.25	6/255	8/255	10/255
MSD	58.43	49.11	41.48	57.13	48.69	39.97
AT ℓ_2	59.75	51.48	45.05	54.37	45.60	37.48
AT ℓ_∞	51.49	38.45	31.47	60.84	53.41	45.83
PAT	55.55	46.19	40.67	51.86	43.19	34.62
Ours	62.39	54.17	46.52	57.81	48.12	38.84

Here, we examine effect of the test time perturbation budget on results that are presented in Table 1 and 2. Although we selected the perturbation bounds according to the prior work in these experiments, we evaluated against other perturbation sizes to give a more comprehensive evaluation of the method. For this purpose, we evaluated a number of methods from Table 1 against PGD attacks with different bounds. Results are shown in Table 5. It shows that if one method is more resistant to an attack with a specific bound than the others, it would also be more resistant against that attack with other bounds. Therefore, this parameter does not have much effect on the final results.

5. Conclusion

Previous works generally examine the robustness only against existing attacks and do not pay attention to unforeseen threat models. This creates a rivalry between defenses and attacks, and for every new defense, a new successful attack emerges, and vice versa. In doing so, we tried to solve this problem and came up with a method that would make the classifier more resistant to unforeseen attacks. To this end, we introduced a new attack that does not have the limitations and biases of previous attacks at the training time and determines the perturbation margin associated with each sample according to the sample itself, using the Lagrangian penalty. Moreover, our introduced method is much faster than others and allows its use for large datasets. Finally, we demonstrated the effectiveness of our method in improving generalization in the CIFAR-10 and ImageNet-100 datasets against many unseen attacks. Our work has shown that using attacks that perform well during test time is not sufficient for training network against unforeseen attacks and it is necessary to design a special teacher for the training time that, in addition to teaching a general case of possible perturbations to the classifier, allows the teacher to determine the allowable amount of perturbation budget for each sample according to the sample itself.

References

- Akhtar, N. and Mian, A. Threat of adversarial attacks on deep learning in computer vision: A survey. *arXiv preprint arXiv:1801.00553*, 2018.
- Andriushchenko, M. and Flammarion, N. Understanding and improving fast adversarial training. In *Advances in Neural Information Processing Systems (NeurIPS)*, 2020.
- Athalye, A., Carlini, N., and Wagner, D. A. Obfuscated gradients give a false sense of security: Circumventing defenses to adversarial examples. In *International Conference on Machine Learning (ICML)*, 2018a.
- Athalye, A., Engstrom, L., Ilyas, A., and Kwok, K. Synthesizing robust adversarial examples. In *International Conference on Machine Learning (ICML)*, 2018b.
- Balaji, Y., Goldstein, T., and Hoffman, J. Instance adaptive adversarial training: Improved accuracy tradeoffs in neural nets. *arXiv preprint arXiv:1910.08051*, 2019.
- Carlini, N. and Wagner, D. Towards evaluating the robustness of neural networks. In *IEEE Symposium on Security and Privacy (SP)*, 2017.
- Chen, T., Liu, S., Chang, S., Cheng, Y., Amini, L., and Wang, Z. Adversarial robustness: From self-supervised pre-training to fine-tuning. In *IEEE Conference on Computer Vision and Pattern Recognition (CVPR)*, 2020.
- Croce, F. and Hein, M. Sparse and imperceivable adversarial attacks. In *International Conference on Computer Vision (ICCV)*, 2019.
- Croce, F. and Hein, M. Reliable evaluation of adversarial robustness with an ensemble of diverse parameter-free attacks. In *International Conference on Machine Learning (ICML)*, 2020.
- Ding, G. W., Sharma, Y., Lui, K. Y. C., and Huang, R. MMA training: Direct input space margin maximization through adversarial training. In *International Conference on Learning Representations (ICLR)*, 2020.
- Dong, Y., Liao, F., Pang, T., Su, H., Zhu, J., Hu, X., and Li, J. Boosting adversarial attacks with momentum. In *IEEE Conference on Computer Vision and Pattern Recognition (CVPR)*, 2018.
- Goodfellow, I. J., Shlens, J., and Szegedy, C. Explaining and harnessing adversarial examples. In *International Conference on Learning Representations (ICLR)*, 2015.
- Ilyas, A., Santurkar, S., Tsipras, D., Engstrom, L., Tran, B., and Madry, A. Adversarial examples are not bugs, they are features. In *Advances in Neural Information Processing Systems (NeurIPS)*, 2019.

- Kang, D., Sun, Y., Hendrycks, D., Brown, T., and Steinhardt, J. Testing robustness against unforeseen adversaries. *arXiv preprint arXiv:1908.08016v2*, 2020.
- Kettunen, M., Härkönen, E., and Lehtinen, J. E-Ipips: Robust perceptual image similarity via random transformation ensembles. *arXiv preprint arXiv:1906.03973*, 2019.
- Kim, M., Tack, J., and Hwang, S. J. Adversarial self-supervised contrastive learning. In *Advances in Neural Information Processing Systems (NeurIPS)*, 2020.
- Krizhevsky, A. and Hinton, G. Learning multiple layers of features from tiny images. Technical report, 2009.
- Kurakin, A., Goodfellow, I. J., and Bengio, S. Adversarial examples in the physical world. In *ICLR Workshop*, 2017.
- Laidlaw, C. and Feizi, S. Functional adversarial attacks. In *Advances in Conference on Neural Information Processing Systems (NeurIPS)*, 2019.
- Laidlaw, C., Singla, S., and Feizi, S. Perceptual adversarial robustness: Defense against unseen threat models. *arXiv preprint arXiv:2006.12655*, 2020.
- Lehman, C. Learning to segment CIFAR10, 2019. URL <https://charlielehman.github.io/post/weak-segmentation-cifar10/>.
- Lin, S. C., Zhang, Y., Hsu, C. H., Skach, M., Haque, M. E., Tang, L., and Mars, J. The architectural implications of autonomous driving: Constraints and acceleration. In *International Conference on Architectural Support for Programming Languages and Operating Systems (ASPLOS)*, 2018.
- Madry, A., Makelov, A., Schmidt, L., Tsipras, D., and Vladu, A. Towards deep learning models resistant to adversarial attacks. In *International Conference on Learning Representations (ICLR)*, 2018.
- Maini, P., Wong, E., and Kolter, J. Z. Adversarial robustness against the union of multiple perturbation models. *arXiv preprint arXiv:1909.04068v2*, 2020.
- Milgrom, P. and Segal, I. Envelope theorems for arbitrary choice sets. *Econometrica*, 70(2):583–601, 2002.
- Modas, A., Moosavi-Dezfooli, S., and Frossard, P. Sparsefool: a few pixels make a big difference. In *IEEE Conference on Computer Vision and Pattern Recognition (CVPR)*, 2019.
- Moosavi-Dezfooli, S., Fawzi, A., and Frossard, P. Deepfool: a simple and accurate method to fool deep neural networks. In *IEEE Conference on Computer Vision and Pattern Recognition (CVPR)*, 2016.
- Rony, J., Hafemann, L. G., Oliveira, L. S., Ayed, I. B., Sabourin, R., and Granger, E. Decoupling direction and norm for efficient gradient-based L2 adversarial attacks and defenses. In *Advances in Neural Information Processing Systems (NeurIPS)*, 2019.
- Rony, J., Granger, E., Pedersoli, M., and Ayed, I. B. Augmented lagrangian adversarial attacks. *arXiv preprint arXiv:2011.11857*, 2020.
- Russakovsky, O., Deng, J., Su, H., Krause, J., Satheesh, S., Ma, S., Huang, Z., Karpathy, A., Khosla, A., Bernstein, M., Berg, A. C., and Fei-Fei, L. ImageNet Large Scale Visual Recognition Challenge. *International Journal of Computer Vision (IJCV)*, 115(3):211–252, 2015. doi: 10.1007/s11263-015-0816-y.
- Szegedy, C., Zaremba, W., Sutskever, I., Bruna, J., Erhan, D., Goodfellow, I., and Fergus, R. Intriguing properties of neural networks. In *International Conference on Learning Representations (ICLR)*, 2014.
- Tramèr, F. and Boneh, D. Adversarial training and robustness for multiple perturbations. In *Advances in Conference on Neural Information Processing Systems (NeurIPS)*, 2019.
- Tsipras, D., Santurkar, S., Engstrom, L., Turner, A., and Madry, A. Robustness may be at odds with accuracy. In *International Conference on Learning Representations (ICLR)*, 2019.
- Uesato, J., O’Donoghue, B., Kohli, P., and van den Oord, A. Adversarial risk and the dangers of evaluating against weak attacks. In *International Conference on Machine Learning (ICML)*, 2018.
- Wang, M. and Deng, W. Deep face recognition: A survey. *arXiv preprint arXiv:1804.06655v9*, 2020.
- Wang, Y., Zou, D., Yi, J., Bailey, J., Ma, X., and Gu, Q. Improving adversarial robustness requires revisiting misclassified examples. In *International Conference on Learning Representations (ICLR)*, 2020.
- Wong, E., Schmidt, F. R., and Kolter, J. Z. Wasserstein adversarial examples via projected sinkhorn iterations. *arXiv preprint arXiv:1902.07906v2*, 2020.
- Xiao, C., Zhu, J.-Y., Li, B., He, W., Liu, M., and Song, D. Spatially transformed adversarial examples. In *International Conference on Learning Representations (ICLR)*, 2018.
- Zagoruyko, S. and Komodakis, N. Paying more attention to attention: Improving the performance of convolutional neural networks via attention transfer. In *International Conference on Learning Representations (ICLR)*, 2017.

Zhang, H., Yu, Y., Jiao, J., Xing, E. P., Ghaoui, L. E., and Jordan, M. I. Theoretically principled trade-off between robustness and accuracy. In *International Conference on Machine Learning (ICML)*, 2019.

Zhang, R., Isola, P., Efros, A. A., Shechtman, E., and Wang, O. The unreasonable effectiveness of deep features as a perceptual metric. In *The IEEE Conference on Computer Vision and Pattern Recognition (CVPR)*, 2018.

Zhou Wang, Bovik, A. C., Sheikh, H. R., and Simoncelli, E. P. Image quality assessment: from error visibility to structural similarity. *IEEE Transactions on Image Processing*, 2004.

A. Flowers recognition

As demonstrated earlier, our method performs better than the others against unseen attacks on CIFAR-10 and ImageNet-100 datasets. Nevertheless, a big concern about all of the methods is that they overfit to these two datasets. In other words, these two datasets have mainly been used for the evaluations, and the satisfactory performance of a method may be limited to these datasets. To address this concern, we examine our method against PGD attacks on another dataset. We set a high bar, by comparing our method against PGD- ℓ_∞ and PGD- ℓ_2 trained model on ℓ_∞ and ℓ_2 balls, respectively.

It is more beneficial to select a dataset with different types of images than the mentioned datasets. It is also preferable that the data be almost balanced and its images have an appropriate resolution. For this purpose, the Flower dataset² is used that contains five different types of flowers (Daisy, Dandelion, Rose, Sunflower, and Tulip). The resolution of the images is about 320x240. This dataset includes some irrelevant images, which we removed for a more accurate evaluation. Looking at the number of samples available in each class in Fig. 6, we realize that the dataset is sufficiently balanced. Some samples in this dataset are shown in Fig. 7.

We trained a ResNet-18 model to classify the flowers using the same training setting as in ImageNet-100. We evaluated it against the PGD attacks with various bounds. Results are shown in Fig. 8 and Fig. 9, which demonstrate the better performance of our method than training with the same attacks being used at the test time. Note the outperforming such baselines is more challenging than comparing with other methods against the unseen attacks.

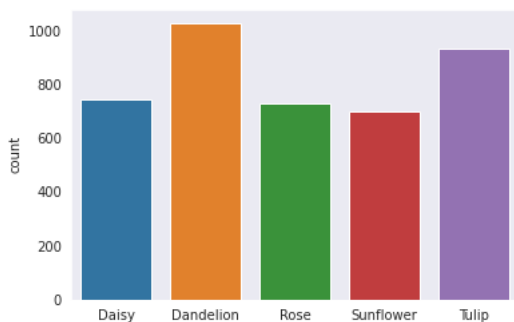


Figure 6. Distribution of various classes in the Flower dataset.

²<https://www.kaggle.com/alxmamaev/flowers-recognition>



Figure 7. Sample images from the Flower dataset. The columns are Daisy, Dandelion, Rose, Sunflower, and Tulip, respectively.

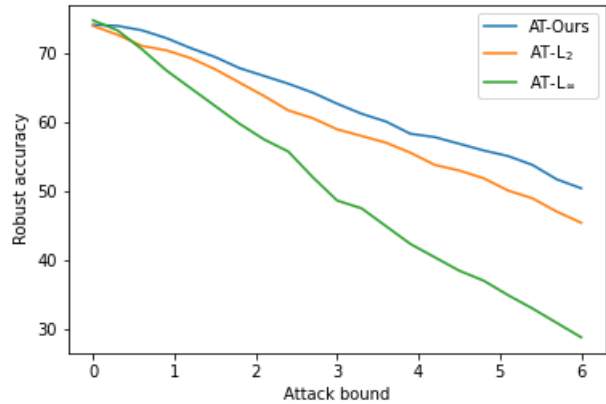


Figure 8. Evaluating adversarially trained models on the Flower dataset against PGD- ℓ_2 with various bounds. Allowable ℓ_2 norm of the perturbation is gradually increased from zero to six.

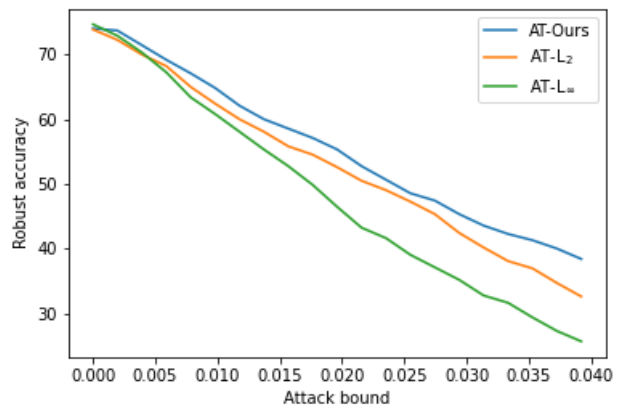


Figure 9. Evaluating adversarially trained models on the Flower dataset against PGD- ℓ_∞ with various bounds. Allowable ℓ_∞ norm of the perturbation is gradually increased from zero to 10/255.

B. Adversarial evaluations

As far as possible, attempts were made to perform the evaluations as comprehensively as possible. Various attacks are used to obtain the robust accuracy of different methods

against unforeseen attacks and attacks used during training to make the assessments entirely fair. Since our context evaluated methods against unseen attacks, we only used PGD- ℓ_∞/ℓ_2 and didn't use stronger versions of PGD. Although if we had used stronger attacks such as AutoAttack (Croce & Hein, 2020), the results would not have changed. To illustrate this point, we checked the accuracy of our method and PAT's method as the method that has the closest clean and unseen accuracy to ours, against standard AutoAttack in CIFAR-10 and ImageNet-100 dataset. The results are reported in Table 6 that demonstrates a similar trend in AutoAttack accuracies to PGD attacks.

Also, to show one aspect of the variety of selected attacks, we examined the average ℓ_2 norm of selected attacks on our CIFAR-10 model, which is reported in Table 7 and shows the chosen attacks' ℓ_2 norm diversity. Furthermore, the slightly larger ℓ_2 norm of the attacks than our training attack is another reason for the selected attacks' fairness. However, it confirms that our contribution is also about removing the LPIPS bias.

Table 6. Comparison of AutoAttack (AA) with PGD (perturbation budgets are similar to Tables 1 and 2). Both show that our model is more robust.

Dataset	Model	ℓ_∞		ℓ_2	
		AA	PGD	AA	PGD
CIFAR-10	Ours	38.47	48.12	44.98	54.17
	PAT	33.75	43.19	39.21	46.19
ImageNet-100	Ours	40.23	46.47	39.80	46.59
	PAT	37.18	43.14	37.51	43.29

Table 7. Average ℓ_2 norm of attacks on our CIFAR-10 model.

Ours	1.31	Elastic	7.87
LPA	2.45	Jpeg	2.07
ℓ_∞	1.56	Noise	12.39
ℓ_2	1.00	Blur	5.68
Recolor	2.18	PGD ₀	7.87
StAdv	3.67		